

Global Inflow and Outflow Solutions (GIOS) around a Black Hole

Sandip K. Chakrabarti

S. N. Bose National Centre For Basic Sciences,
JD Block, Salt Lake, Sector-III, Calcutta-700091
e-mail: chakraba@boson.bose.res.in

Abstract

Twenty five years have passed by since models of accretions and jets have separately emerged. Today, it is understood that these two objects are related to each other in a fundamental way. In a binary system, matter from an accretion disk enters into a black hole. A part of it is bounced back because of the centrifugal barrier, radiation pressure or magnetohydrodynamic effects, to form jets and bipolar outflows which carry away excess angular momentum. In the case of AGNs containing black holes, accretion disks form out of stellar winds and similar processes as above form cosmic radio jets. We present a general review of the study of the accretion disks and outflows in a coherent manner, especially emphasizing global inflow-outflow solutions (GIOS). We also present a few observational consequences of wind production from the accretion disks on spectral properties of the accretion disks.

To appear in the proceedings of the Mini Workshop on Fluid Dynamics at the Dacca University (August, 1998). Ed. A. Hosain.

1 Introduction

Study of accretion disks and outflows around black holes began twenty-five years ago [1-2]. The subject has evolved considerably since then and it is now clear that these two apparently dissimilar objects are related to each other. The accretion solutions of purely rotating disk have been improved to include the effect of radiation pressure [3-7] (See Chakrabarti [8] for a review.). Jet solutions have changed from speculative ideas such as de-Laval nozzles [9] to electro-dynamically acceleration model [10], self-similar centrifugally driven outflows [11], ‘cauldrons’ [12] etc. Centrifugally driven outflows are subsequently modified to include accretion disks [13]. Chakrabarti & Bhaskaran [14] (see also, Contopoulos, [15]) showed that it is easier produce outflows from a sub-Keplerian inflow.

Parallely, efforts were on to study the accretion and jets within the same framework. Chakrabarti [16-17] found that the same solution of purely rotating flows around a black hole could describe accretion flows on the equatorial plane and pre-jet matters near the axis. With a natural angular momentum distribution of $l(r) = c\lambda(r)^n$, (where c and n are constants and λ is the von Zeipel parameter) it was found that for large c and small n ($n < 1$), solutions are regular on the equatorial plane and they describe thick accretion disks. For small c and large n ($n > 1$), the solutions are regular on the axis and they describe pre-jet matters. It was speculated that some viscous process might be responsible to change the parameters from one set to the other. Even in the absence of viscosity, constant angular momentum flow was found to bounce back from the centrifugal barrier in numerical simulations of accretion flows [18]. Eggum, Coroniti & Katz [19] considered radiatively outflows emerging from a Keplerian disk.

Further progress of this topic required a fundamental understanding of these flows which emerged in the late 1980s. It was found out just as Bondi solution [20] of accretion onto stars is related to outflow solutions [21], fundamentally transonic black hole accretions and winds are also related to each other. All possible accretion and wind type solutions are found,

including solutions which may contain standing shocks and the entire parameter space is classified according to the nature of solutions [22-23]. Fig. 1 (taken from Chakrabarti, [24]) shows these solutions (Mach number is plotted against logarithmic radial distance [in Units of the Schwarzschild Radius] and outer boxes, and specific energy is plotted against specific angular momentum in the central box) and the classification of the parameter space when the Kerr parameter $a = 0.5$ and when the equatorial plane solutions are considered (similar solutions are present for conical flows in winds as well, see [23]). The inward pointing arrows indicate accretion solutions and the outward pointing arrows indicate wind solutions. The flow from regions I, O pass through the inner sonic point and outer sonic point respectively. Those from NSA have no shock in accretion, from SA have shocks in accretion, from NSW have no shocks in winds, and SW have shocks in winds respectively. The Global Inflow Outflow Solutions (GIOS) as will be described in §3 combine one solution of each kind to produce wind out of accretion. The horizontal line in the central box denotes the rest mass of the inflow. Note that the outflows are produced only when the specific energy is higher than the rest mass energy. Flow with with lesser energy produces solutions with closed topologies (I* and O*). When viscosity was added the nature of the solutions changed fundamentally [25] (see, [26-27] for details) allowing matter to directly come out of a Keplerian disk and enter into a black hole through the sonic point. These solutions, both for the accretion and winds have been verified by complete time-dependent simulations [28-31]. In the case of steady state solutions, outflows are found to occur between the centrifugal barrier and the funnel wall (Fig. 2a below) while in a non-steady solution the outflow could spread in regions outside the centrifugal barrier as well.

2 Recent Progresses in Accretion Disk Solutions

Fig. 2a shows the general picture that emerges of the non-magnetized inflow and outflow around a black hole. Centrifugal force tends to fight against gravity close to a black hole to produce a denser region called CENBOL (centrifugal barrier supported boundary layer). Matter farther out rotates in a Keplerian disk, but close to the black hole the flow is puffed up due to radiation pressure or ion pressure depending on whether the accretion rate is sufficiently high or not. The two-dimensional nature of the density distribution is given in Chakrabarti [24].

Chakrabarti & Titarchuk [32] using this generalized accretion solution suggested that hard and soft states of a black hole could be understood simply by re-distribution of matter between Keplerian and sub-Keplerian components which is effected by variation of viscosity in the flow in the vertical direction. This general conclusions is verified observationally (Zhang et al. 1997). The constancy of energy spectral index α_e ($F_\nu \propto \nu^{-\alpha_e}$) separately in hard and soft states, as well as possible shifting of the inner edge with the Keplerian component with accretion rate as predicted by the general accretion solution [26] have also been verified [34-36]. It was also recognized that the non-stationary solutions of the accretion flows [37-38] might cause quasi-periodic oscillations. It was pointed out that the outflows, and not accretion disks, could be responsible for the Iron K_α lines and the so-called reflection components [32]. A schematic representation of the detailed picture as above is drawn in Fig. 2b. We shall use this picture below to analytically estimate the outflow rates.

A new concept which was found useful in identifying black holes by using spectral features alone is the ‘bulk motion Comptonization’. Basically, as matter flows into a black hole rapidly with almost the speed of light, photons scattering from them gain momentum and frequency is blue-shifted due to Doppler effect [32, 39]. The resulting spectra is of power-law and extends till about an MeV. The presence of this part of the spectra in soft states is widely accepted to be the only way to identify a black hole most convincingly, whether

galactic or extragalactic, since the all absorbing property of the horizon is directly used in obtaining the spectral slope.

Black holes in X-ray binaries often show quiescence states. This could be the result of very low accretion rates. A novel solution that was proposed by Das & Chakrabarti [40] (also see, [41-42]) is that outflows generated from the inflow could, in some certain circumstances especially when the accretion rate is low, be so high that the disk may be almost evacuated. They proposed that such outflows could generate quiescence states of a black hole candidate.

3 Global Inflow-Outflow Solutions (GIOS)

Outflows are common in many astrophysical systems which contain black holes and neutron stars. Difference between stellar outflows and outflows from these systems is that the outflows in these systems have to form out of the inflowing material only. We now present a simple analytical approach by which the outflow rate is computed out of the inflow rate. The ratio of these two rates is found to be a function the compression ratio of the gas at the boundary between CENBOL and the inflow.

The problem of mass outflow rate in the context of a black hole accretion has been attacked quite recently [27, 43]. A simple approach widely used in stellar astrophysics has been followed where the flow upto the sonic point is assumed to be isothermal. This was possible due to the novel understanding that around a black hole, the centrifugal pressure supported dense matter could behave like a ‘boundary layer’. This CENBOL is hot, puffed up and very similar to the classical thick accretion disk, except that at the inner edge the matter is strongly advective. The thermal pressure is expected to drive matter out in between the centrifugal barrier and the funnel wall [31] as in Fig 2a. However, we use a simple model (Fig. 2b) where both the inflow is axially symmetric and wedge shaped while the outflow is conical with solid angles Θ_{in} and Θ_{out} respectively.

CENBOL could form either with or without shocks as long as the angular momentum of the flow close to the compact object is roughly constant as is the case in reality [22-24]. This region replaces [32, 44-45] the so called ‘Compton cloud’ in explaining hard and soft states of black hole. The oscillation of this region can explain the general properties of the quasi-periodic oscillation [37,38,46] from black holes and neutron stars. It is therefore of curiosity if this region plays any major role in formation of outflows.

Several authors have also mentioned of denser regions closer to a black hole due to different physical effects. Chang & Ostriker [47] showed that pre-heating of the gas could produce standing shocks at a large distance (typically a few tens of thousands Schwarzschild radii away). Kazanas & Ellison [48] mentioned that pressure due to pair plasma could produce standing shocks at smaller distances around a black hole as well. Our computation is insensitive to the actual mechanism by which the boundary layer is produced. All we require is that the gas should be hot at the region where the compression takes place. Thus, since Comptonization processes cool this region [32] for larger accretion rates ($\dot{M} \gtrsim 0.1\dot{M}_{Eddington}$) our process is valid only for low-luminosity objects, consistent with current observations. Begelman & Rees [12] talked about a so-called ‘cauldron’ model of compact objects where jets were assumed to emerge from a dense mixture of matter and radiation by boring a de-Laval nozzle as in Blandford & Rees [9] model. The difference between this model and the present one is that very high accretion rate was required ($\dot{M}_{in} \sim 1000\dot{M}_E$) there while we consider thermally driven outflows out of accretion with smaller rates. Second, the size of the ‘cauldron’ was thousands of Schwarzschild radii (where gravity was so weak that channel has to have shape of a de-Laval nozzle to produce transonicity), while we have a CENBOL of about $10R_g$ (where the gravity plays an active role in creating the transonic wind) in our mind. Third, in the present case, matter is assumed to pass through a sonic point

using the pre-determined funnel where rotating pre-jet matter is accelerated [16] and not through a ‘bored nozzle’ even though symbolically a quasi-spherical CENBOL is considered for mathematical convenience.

Once the presence of the centrifugal pressure supported boundary layer (CENBOL) is accepted, the mechanism of the formation of the outflow becomes clearer. One basic criteria is that the outflowing winds should have positive Bernoulli constant [22]. Just as photons from the stellar surface deposit momentum on the outflowing wind and keeps the flow roughly isothermal [49] at least upto the sonic point, one may assume that the outflowing wind close to the black hole is kept isothermal due to deposition of momentum from hard photons. In the case of the sun, it’s luminosity is only $10^{-5} L_{Edd}$ and the typical mass outflow rate from the solar surface is $10^{-14} M_{\odot} \text{ year}^{-1}$ [50]. Proportionately, for a star with a Eddington luminosity, the outflow rate would be $10^{-9} M_{\odot} \text{ year}^{-1}$. This is roughly half as the Eddington rate for a stellar mass star. Thus if the flow is compressed and heated at the centrifugal barrier around a black hole, it would also radiate enough to keep the flow isothermal (at least up to the sonic point) if the efficiency were exactly identical. Physically, both requirements may be equally difficult to meet, but in reality with photons shining on outflows near a black hole with almost 4π solid angle (from funnel wall) it is easier to maintain the isothermality in the slowly moving (subsonic) region in the present context. Another reason is this: the process of momentum deposition on electrons is more efficient near a black hole. The electron density n_e falls off as $r^{-3/2}$ while the photon density n_{γ} falls off as r^{-2} . Thus the ratio $n_e/n_{\gamma} \propto r^{1/2}$ increases with the size of the region. Thus a compact object will have lesser number of electrons per photon and the momentum transfer is more efficient. In a simpler minded way the physics is scale-invariant, though. In solar physics, it is customary to chose a momentum deposition term which keeps the flow isothermal to be of the form [51],

$$F_r = \int_{R_s}^r D dr$$

where, D is the momentum deposition (localized around r_p) factor with a typical spatial dependence,

$$D = D_0 e^{-\alpha(r/r_p-1)^2}$$

Here, D_0 , α are constants and R_s is the location of the stellar surface. Since r and r_p comes in ratio, exactly same physical consideration would be applicable to black hole physics, with the same result *provided* D_0 is scaled with luminosity (However, as we showed above, D_0 goes up for a compact object due to higher solid angle.). However, as Chakrabarti & Titarchuk [32] showed, high accretion rate ($\dot{M} \gtrsim 0.3 \dot{M}_{Edd}$) will *reduce* the temperature of the CENBOL catastrophically, and therefore our assumption of isothermality of the outflow would severely breakdown at these high rates simply because cooler outflow would have sonic point very far away from the black hole. It is to be noted that in the context of stellar physics, it is shown [52] that the temperature stratification in the outflowing wind has little effect on the mass loss rate. Effect of radiation momentum deposition on the topology of the outflows is separately discussed in Chattopadhyay [53].

3.1 Derivation of the outflow rate using simple GIOS

The accretion rate of the incoming accretion flow is given by,

$$\dot{M}_{in} = \Theta_{in} \rho \vartheta r^2. \quad (1)$$

Here, Θ_{in} is the solid angle subtended by the inflow, ρ and ϑ are the density and velocity respectively, and r is the radial distance. For simplicity, we assume geometric units ($G = 1 = M_{BH} = c$; G is the gravitational constant, M_{BH} is the mass of the central black hole,

and c is the velocity of light) to measure all the quantities. In this unit, for a freely falling gas,

$$\vartheta(r) = \left[\frac{1 - \Gamma}{r} \right]^{1/2} \quad (2)$$

and

$$\rho(r) = \frac{\dot{M}_{in}}{\Theta_{in}} (1 - \Gamma)^{-1/2} r^{-3/2} \quad (3)$$

Here, Γ/r^2 (with Γ assumed to be a constant) is the outward force due to radiation.

We assume that the boundary of the denser cloud is at $r = r_s$ (typically a few Schwarzschild radii, see, Chakrabarti [24]) where the inflow gas is compressed. The compression could be abrupt due to standing shock or gradual as in a shock-free flow with angular momentum. This details are irrelevant. At this barrier, then

$$\rho_+(r_s) = R\rho_-(r_s) \quad (4a)$$

and

$$\vartheta_+(r_s) = R^{-1}\vartheta_-(r_s) \quad (4b)$$

where, R is the compression ratio. Exact value of the compression ratio is a function of the flow parameters, such as the specific energy and the angular momentum (e.g., [22-24]) Here, the subscripts $-$ and $+$ denote the pre-shock and post-shock quantities respectively. At the shock surface, the total pressure (thermal pressure plus ram pressure) is balanced.

$$P_-(r_s) + \rho_-(r_s)\vartheta_-^2(r_s) = P_+(r_s) + \rho_+(r_s)\vartheta_+^2(r_s). \quad (5)$$

Assuming that the thermal pressure of the pre-shock incoming flow is negligible compared to the ram pressure, using eqs. 4(a-b) we find,

$$P_+(r_s) = \frac{R-1}{R} \rho_-(r_s)\vartheta_-^2(r_s). \quad (6)$$

The isothermal sound speed in the post-shock region is then,

$$C_s^2 = \frac{P_+}{\rho_+} = \frac{(R-1)(1-\Gamma)}{R^2} \frac{1}{r_s} = \frac{(1-\Gamma)}{f_0 r_s} \quad (7)$$

where, $f_0 = R^2/(R-1)$. An outflow which is generated from this dense region with very low flow velocity along the axis is necessarily subsonic in this region, however, at a large distance, the outflow velocity is expected to be much higher compared to the sound speed, and therefore the flow must be supersonic. In the subsonic region of the outflow, the pressure and density are expected to be almost constant and thus it is customary to assume isothermality condition up to the sonic point [49]. With isothermality assumption or a given temperature distribution ($T \propto r^{-\beta}$ with β a constant; see eq. [22] below) the result is derivable in analytical form. The sonic point conditions are obtained from the radial momentum equation,

$$\vartheta \frac{d\vartheta}{dr} + \frac{1}{\rho} \frac{dP}{dr} + \frac{1-\Gamma}{r^2} = 0 \quad (8)$$

and the continuity equation

$$\frac{1}{r^2} \frac{d(\rho\vartheta r^2)}{dr} = 0 \quad (9)$$

in the usual way, i.e., by eliminating $d\rho/dr$,

$$\frac{d\vartheta}{dr} = \frac{N}{D} \quad (10)$$

where

$$N = \frac{2C_s^2}{r} - \frac{1-\Gamma}{r^2}$$

and

$$D = \vartheta - \frac{C_s^2}{\vartheta}$$

and putting $N = 0$ and $D = 0$ conditions. These conditions yield, at the sonic point $r = r_c$, for an isothermal flow,

$$\vartheta(r_c) = C_s. \quad (11a)$$

and

$$r_c = \frac{1-\Gamma}{2C_s^2} = \frac{f_0 r_s}{2} \quad (11b)$$

where, we have utilized eq. (7) to substitute for C_s .

Since the sonic point of a hotter outflow is located closer to the black hole, clearly, the condition of isothermality is best maintained if the temperature is high enough. However if the temperature is too high, so that $r_c < r_s$, one has to solve this case more carefully, using considerations of Fig. 2a, rather than of Fig. 2b.

The constancy of the integral of the radial momentum equation (eq. 8) in an isothermal flow gives:

$$C_s^2 \ln \rho_+ - \frac{1-\Gamma}{r_s} = \frac{1}{2} C_s^2 + C_s^2 \ln \rho_c - \frac{1-\Gamma}{r_c} \quad (12)$$

where, we have ignored the initial value of the outflowing radial velocity $\vartheta(r_s)$ at the dense region boundary ($r = r_s$), and also used eq. (11a). We have also put $\rho(r_c) = \rho_c$ and $\rho(r_s) = \rho_+$. Upon simplification, we obtain,

$$\rho_c = \rho_+ \exp(-f) \quad (13)$$

where,

$$f = f_0 - \frac{3}{2}$$

Thus, the outflow rate is given by,

$$\dot{M}_{out} = \Theta_{out} \rho_c \vartheta_c r_c^2 \quad (14)$$

where, Θ_{out} is the solid angle subtended by the outflowing cone. Upon substitution, one obtains,

$$\frac{\dot{M}_{out}}{\dot{M}_{in}} = R_{in} = \frac{\Theta_{out}}{\Theta_{in}} \frac{R}{4} f_0^{3/2} \exp(-f) \quad (15)$$

which, explicitly depends only on the compression ratio:

$$\frac{\dot{M}_{out}}{\dot{M}_{in}} = R_{in} = \frac{\Theta_{out}}{\Theta_{in}} \frac{R}{4} \left[\frac{R^2}{R-1} \right]^{3/2} \exp\left(\frac{3}{2} - \frac{R^2}{R-1}\right) \quad (16)$$

apart from the geometric factors. Notice that this simple result does not depend on the location of the sonic points or the the size of the dense cloud or the outward radiation force constant Γ . This is because the Newtonian potential was used throughout and the radiation force was also assumed to be very simple minded (Γ/r^2). Also, effects of centrifugal force was ignored. Similarly, the ratio is independent of the mass accretion rate which should be valid only for low luminosity objects. For high luminosity flows, Comptonization would cool the dense region completely [32] and the mass loss will be negligible. Pair plasma supported quasi-spherical shocks forms for low luminosity as well [48]. In reality there

would be a dependence on these quantities when full general relativistic considerations of the rotating flows are made. Exact and detailed computations using both the transonic inflow and outflow (where the compression ratio R is also computed self-consistently) are presented elsewhere [40].

Figure 3 contains the basic results. The solid curve shows the ratio $R_{\dot{m}}$ as a function of the compression ratio R (plotted from 1 to 7), while the dashed curve shows the same quantity as a function of the polytropic constant $n = (\gamma - 1)^{-1}$ (drawn from $n = 3/2$ to 3), γ being the adiabatic index. The solid curve is drawn for any generic compression ratio and the dashed curve is drawn assuming the strong shock limit only: $R = (\gamma + 1)/(\gamma - 1) = 2n + 1$. In both the curves, $\Theta_{out} \sim \Theta_{in}$ has been assumed for simplicity. Note that if the compression does not take place (namely, if the denser region does not form), then there is no outflow in this model. Indeed for, $R = 1$, the ratio $R_{\dot{m}}$ is zero as expected. Thus the driving force of the outflow is primarily coming from the hot and compressed region. The basic form is found to agree with results obtained from rigorous calculation with transonic inflow and outflow.

In a relativistic inflow or for a radiation dominated inflow, $n = 3$ and $\gamma = 4/3$. In the strong shock limit, the compression ratio is $R = 7$ and the ratio of inflow and outflow rates becomes,

$$R_{\dot{m}} = 0.052 \frac{\Theta_{out}}{\Theta_{in}}. \quad (17a)$$

For the inflow of a mono-atomic ionized gas $n = 3/2$ and $\gamma = 5/3$. The compression ratio is $R = 4$, and the ratio in this case becomes,

$$R_{\dot{m}} = 0.266 \frac{\Theta_{out}}{\Theta_{in}}. \quad (17b)$$

Since f_0 is smaller for $\gamma = 5/3$ case, the density at the sonic point in the outflow is much higher (due to exponential dependence of density on f_0 , see, eq. 7) which causes the higher outflow rate, even when the actual jump in density in the postshock region, the location of the sonic point and the velocity of the flow at the sonic point are much lower. It is to be noted that generally for $\gamma > 1.5$ shocks are not expected [23], but the centrifugal barrier supported dense region would still exist. As is clear, the entire behavior of the outflow depends only on the compression ratio, R and the collimating property of the outflow Θ_{out}/Θ_{in} .

Outflows are usually concentrated near the axis, while the inflow is near the equatorial plane. Assuming a half angle of 10° in each case, we obtain,

$$\Theta_{in} = \frac{2\pi^2}{9}; \quad \Theta_{out} = \frac{\pi^3}{162}$$

and

$$\frac{\Theta_{out}}{\Theta_{in}} = \frac{\pi}{36}. \quad (18)$$

The ratios of the rates for $\gamma = 4/3$ and $\gamma = 5/3$ are then

$$R_{\dot{m}} = 0.0045 \quad (19a)$$

and

$$R_{\dot{m}} = 0.023 \quad (19b)$$

respectively. Thus, in quasi-spherical systems, in the case of strong shock limit, the outflow rate is at the most a couple of percent of the inflow. If this assumption is dropped, then for a cold inflow, the rate could be higher by about fifty percent (see, Fig. 3).

It is to be noted that the above expression for the outflow rate is strictly valid if the flow could be kept isothermal at least up to the sonic point. In the event this assumption

is dropped the expression for the outflow rate becomes dependent on several parameters. As an example, we consider a polytropic outflow of same index γ but of a different entropy function K (We assume the equation of state to be $P = K\rho^\gamma$, with $\gamma \neq 1$). The expression (11b) would be replaced by,

$$r_c = \frac{f_0 r_s}{2\gamma} \quad (20)$$

and eq. (12) would be replaced by,

$$na_+^2 - \frac{1-\Gamma}{r_s} = \left(\frac{1}{2} + n\right)a_s^2 - \frac{1-\Gamma}{r_c} \quad (21)$$

where $n = 1/(\gamma - 1)$ is the polytropic constant of the flow and $a_+ = (\gamma P_+/\rho_+)^{1/2}$ and $a_c = (\gamma P_c/\rho_c)^{1/2}$ are the adiabatic sound speeds at the starting point and the sonic point of the outflow. It is easily shown that a power law temperature fall off of the outflow ($T \propto r^{-\beta}$) would yield

$$R_{\dot{m}} = \frac{\Theta_{out}}{\Theta_{in}} \left(\frac{K_i}{K_o}\right)^n \left(\frac{f_0}{2\gamma}\right)^{\frac{3}{2}-\beta}, \quad (22)$$

where, K_i and K_o are the entropy functions of the inflow and the outflow. This derivation is strictly valid for a non-isothermal flow. Since $K_i < K_o$, $n > 3/2$ and f_0 , for $\Theta_{out} \sim \Theta_{in}$, $R_{\dot{m}} \ll 1$ is guaranteed provided $\beta > \frac{3}{2}$, i.e., if the temperature falls for sufficiently rapidly. For an isothermal flow $\beta = 0$ and the rate tends to be higher. Note that since $n \sim \infty$ in this case, any small jump in entropy due to compression will off-balance the the effect of $f_0^{-3/2}$ factor. Thus $R_{\dot{m}}$ remains smaller than unity. The first factor decreases with entropy jump while the second factor increases with the compression ratio (R) when $\beta < 3/2$. Thus the solution is still expected to be similar to what is shown in Fig. 3.

3.2 Results from Rigorously obtained GIOS

When inflow and outflow solutions are obtained more rigorously, i.e., actually making the flow pass through separate sonic surfaces, one has to include the effect of mass-loss on the Rankine-Hugoniot condition at the boundary between CENBOL and the accretion flow [40]. Accordingly, we use,

$$\dot{M}_+ = (1 - R_{\dot{m}})\dot{M}_- \quad (23)$$

where, the subscripts $+$ and $-$ denote the pre- and post-shock values respectively. Since due to the loss of matter in the post-shock region, the post-shock pressure goes down, the shock recedes backward for the same value of incoming energy, angular momentum & polytropic index. The combination of three changes, namely, the increase in the cross-sectional area of the outflow and the launching velocity of the outflow and the decrease in the post-shock density decides whether the net outflow rate would increased or decreased than from the case when the exact Rankine-Hugoniot relation was used.

Fig. 4 shows a typical global inflow-outflow solution (GIOS) where actual transonic problem was solved. The input parameters are $\mathcal{E} = 0.0005$, $\lambda = 1.75$ and $\gamma = 4/3$ corresponding to relativistic inflow. The solid curve with an arrow represents the pre-shock region of the inflow and the long-dashed curve represents the post-shock inflow which enters the black hole after passing through the inner sonic point (I). The solid vertical line at X_{s3} (the left-most vertical transition; the notation of the shock location is from [22]) with double arrow represents the shock transition obtained with exact Rankine-Hugoniot condition (i.e., with no mass loss). The actual shock location obtained with modified Rankine-Hugoniot condition (eq. 23) is farther out from the original location X_{s3} . Three vertical lines connected with the corresponding dotted curves represent three outflow solutions for the parameters $\gamma_o = 1.3$ (top), 1.15 (middle) and 1.05 (bottom). The outflow branches shown pass through

the corresponding sonic points. It is evident from the figure that the outflow moves along solution curves which are completely different from that of the ‘wind solution’ of the inflow which passes through the outer sonic point ‘O’. The mass loss ratio $R_{\dot{m}}$ in these cases are 0.256, 0.159 and 0.085 respectively. This figure is taken from [40]. Fig. 3 of that work shows the general behaviour of the variation of $R_{\dot{M}}$ with compression ratio of the shock. This agrees well with what is obtained analytically (Fig. 3 of this paper).

Das & Chakrabarti [40], for the first time, pointed out that in certain region of the parameter space, the mass loss could be so much that disk would be almost evacuated and conjectured that inactive phases of a black hole (such as the present day Sgr A* at our galactic center) may be formed when such profuse mass loss takes place.

It is to be noted that although the existence of outflows are well known, their rates are not. The only definite candidate whose outflow rate is known with any certainty is probably SS433 whose mass outflow rate was estimated to be $\dot{M}_{out} \gtrsim 1.6 \times 10^{-6} f^{-1} n_{13}^{-1} D_5^2 M_{\odot} \text{ yr}^{-1}$ [54], where f is the volume filling factor, n_{13} is the electron density n_e in units of 10^{13} cm^{-3} , D_5 is the distance of SS433 in units of 5kpc. Considering a central black hole of mass $10M_{\odot}$, the Eddington rate is $\dot{M}_{Ed} \sim 0.2 \times 10^{-7} M_{\odot} \text{ yr}^{-1}$ and assuming an efficiency of conversion of rest mass into gravitational energy $\eta \sim 0.06$, the critical rate would be roughly $\dot{M}_{crit} = \dot{M}_{Ed}/\eta \sim 3.2 \times 10^{-7} M_{\odot} \text{ yr}^{-1}$. Thus, in order to produce the outflow rate mentioned above even with our highest possible estimated $R_{\dot{m}} \sim 0.4$ (see, Fig. 2), one must have $\dot{M}_{in} \sim 12.5 \dot{M}_{crit}$ which is very high indeed. One possible reason why the above rate might have been over-estimated would be that below 10^{12} cm from the central mass [54], $n_{13} \gg 1$ because of the existence of the dense region at the base of the outflow.

In numerical simulations the ratio of the outflow and inflow has been computed in several occasions [19,29]. Eggum et al. [19] found the ratio to be $R_{\dot{m}} \sim 0.004$ for a radiation pressure dominated flow. This is generally comparable with what we found above (eq. 19a). In Molteni et al. [29] the centrifugally driven outflowing wind generated a ratio of $R_{\dot{m}} \sim 0.1$. Here, the angular momentum was present in both inflow as well as outflow, and the shock was not very strong. Thus, the result is again comparable with what we find here.

3.3 Spectral Softening in Presence of Profuse Mass Loss

Creation of winds out of accretion disk has an interesting consequence. As more fraction of matter is expelled, it becomes easier for the soft photons from the Keplerian disk (see Fig. 2a) surrounding the advective region to cool this region due to Comptonization (see, Chakrabarti & Titarchuk for details). In other words, the presence of winds would *soften* the spectra of the power-law component for the *same* multicolour blackbody component. Such an observation would point to profuse mass loss from the hot advective region.

The model we use here is the two component accretion flow which has a CENBOL close to the hole. We assume a weakly viscous flow of constant specific angular momentum $\lambda = 1.75$ (in units of $2GM/c$) for the sake of concreteness. The Keplerian component close to the equatorial plane has a low accretion rate ($\dot{M}_{in} \sim 0.05 - 0.3$ in units of the Eddington rate) and the sub-Keplerian halo surrounding it has a higher rate ($\dot{M}_h \sim 1$ in units of Eddington rate). Before the accreting matter hits the inner advective region, both the rates are constant, but as Das & Chakrabarti [40] has shown, winds, produced from CENBOL will deplete the disk matter at the rate determined by the temperature of the CENBOL, when other parameters, such as the specific angular momentum and specific energy are kept fixed.

Figures 5 and 6 show the outcome of our calculation of the spectra for three different accretion rate of the Keplerian component \dot{M}_{in} [43]. The mass of the central black hole is chosen to be $M = 10M_{\odot}$. The size of the CENBOL is assumed to be $10r_g$ (where r_g is the Schwarzschild radius), a typical location for the sub-Keplerian flow of average specific

angular momentum $\lambda = 1.75$ and specific energy $\mathcal{E} = 0.003$. Following Das & Chakrabarti [40], we first compute the mass outflow rate from the advective region. The long dashed curve in Fig. 5 shows the variation of the percentage of mass loss (vertical axis on the right) as a function of the inflow accretion rate. The dotted curve and the solid curve denote the variation of the energy spectral index α ($F_\nu \propto \nu^{-\alpha}$) with and without winds taken into account. Note that the spectra is overall softened (α increased) when winds are present. For higher Keplerian rates, the mass loss through winds is negligible and therefore there is virtually no change in the spectral index. For lower inflow rates, on the other hand, mass loss rate is more than twenty percent. It is easier to Comptonize the depleted matter by the same number of incoming soft photons and therefore the spectra is softened.

In Fig. 6, we show the resulting spectral change. As in Fig. 5, solid curves represent solutions without winds and the dotted curves represent solutions with winds. Solid curves are drawn for $\dot{M}_{in} = 0.3$ (uppermost at the bump), 0.15 (middle at the bump) and 0.07 (lowermost at the bump) respectively. For $\dot{M}_{in} = 0.3$ both curves are identical. Note the crossing of the solid curves at around $10^{18.6} Hz$ (15 keV) when winds are absent. This is regularly observed in black hole candidates. If this is shifted to higher energies, the presence of winds may be indicated.

Strong winds are suspected to be present in Sgr A* at our Galactic Center (see, Genzel et al. [55] for a review, and Eckart & Genzel [56]). Chakrabarti [9] suggested that the inflow could be of almost constant energy transonic flow, so that the emission is inefficient. However, from global inflow-outflow solutions [GIOS], Das & Chakrabarti [40] showed that when the inflow rate itself is low (as is the case for Sgr A*; $\sim 10^{-3}$ to $10^{-4} \dot{M}_{Eddington}$) the mass outflow rate is very high, almost to the point of evacuating the disk. This prompted them to speculate that spectral properties of our Galactic Center could be explained by inclusion of winds. This will be done in near future. Not only our Galactic Center, the consideration should be valid for all the black hole candidates (e.g., V404 Cyg) which are seen in quiescence.

Chakrabarti & Titarchuk [32] suggested that the iron K_α line as well as the so called ‘reflection component’ could be due to outflows off the advective region. Combined with the present work, we may conclude that simultaneous enhancement of the ‘reflection component’ and/or iron K_α line intensity with the softening of the spectra in hard X-rays would be a sure signature of the presence of significant winds in the advective region of the disk.

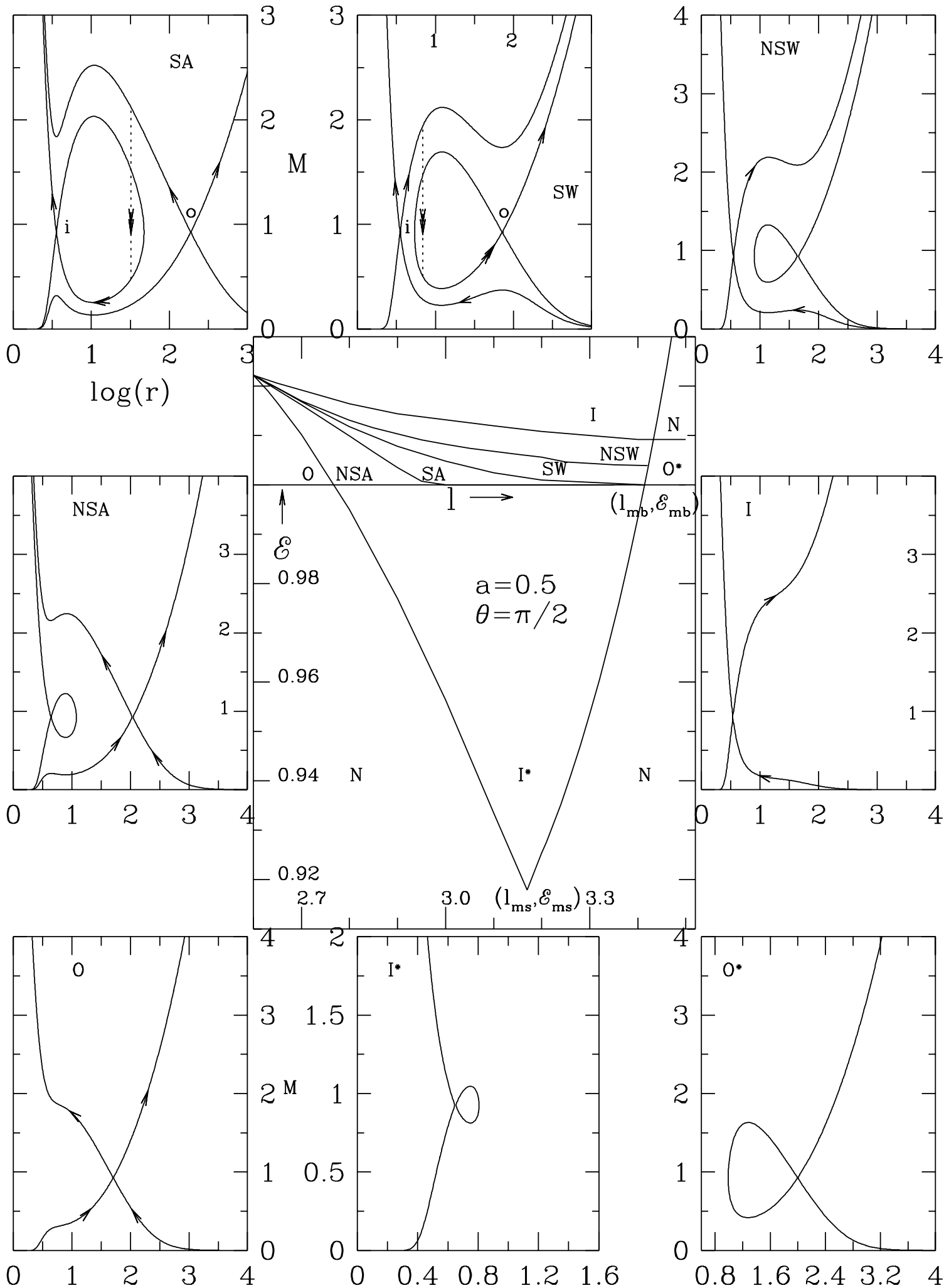
References

1. Shakura, N.I. & Sunyaev, R.A. 1973, Black holes in binary systems: Observational appearance, *Astr. Ap.*, **24**, 337-355
2. Longair, M.S., Ryle, M. & Scheuer, P.A.G., 1973, Models of extended radio sources, *Mon. Not. R. Astron. Soc.* **164**, 243-250
3. Maraschi, L., Reina C., & Treves, A., 1976, The effect of radiation pressure on accretion disks around black holes, *Astrophys. J.* **206**, 295-300
4. Paczyński B. & Wiita, P.J., 1980, Thick accretion disks and supercritical luminosities, *Astron. Ap.* **88**, 23-31
5. Liang E.P.T. & Thompson, K.A. 1980, Transonic disk accretion onto black holes, *Astrophys. J.*, **240**, 271-274
6. Paczyński B. & Bisnovatyi-Kogan, G. 1981, *Acta Astron.* **31**, 283-293
7. Muchotrzeb B., & Paczyński, B. 1982, Transonic accretion flow in a thin disk around a black hole, *Acta Astron.* **32**, 1-11
8. Chakrabarti, S. K. 1996, in *Accretion Processes on Black Holes*, *Physics Reports*, **266**, No. 5 & 6, p. 229-390
9. Blandford, R.D. & Rees, M.J. 1974, A 'twin-exhaust' model for double radio sources, *Mon. Not. R. Astro. Soc.*, **169**, 395-415
10. Znajek, R.L., 1978, Charged current loops around Kerr holes, *Mon. Not. R. Astron. Soc.*, **182**, 639-646
11. Blandford R.D. & Payne, D.G. 1981, Hydromagnetic flows from accretion discs and the production of radio jets, *Mon. Not. R. Astron. Soc.* **194**, 883-903
12. Begelman, M.C. & Rees, M.J., 1984, The cauldron at the core of SS 433, *Mon. Not. R. Astro. Soc.*, **206**, 209-220
13. Königl, A. 1989, Self-similar models of magnetized accretion disks, *Astrophys. J.*, **342**, 208-223
14. Chakrabarti, S.K. & Bhaskaran, P. 1992, *Mon. Not. R. Astron. Soc.* **255**, 255-260
15. Contopoulos, J. 1995, Force-free Self-similar Magnetically Driven Relativistic Jets *Astrophys. J.*, **446**, 67-74
16. Chakrabarti, S.K. 1984 in *Active Galactic Nuclei*, ed. J. Dyson, (Manchester University Press), 346-350
17. Chakrabarti, S.K., 1985 *Astrophys. J.* **288**, 7-13
18. Hawley, J.W., Wilson, J. & Smarr, L. 1984, A numerical study of nonspherical black hole accretion: I- Equations and test problems, *Astrophys. J.*, **277**, 296-311
19. Eggum, G. E., Coroniti, F. V., Katz, J. I. 1985, Jet production in super-Eddington accretion disks, *Astrophys. J.*, **298**, L41-L45
20. Bondi, H. 1952, On Spherically Symmetrical Accretion, *Mon. Not. R. Astron. Soc.* **112**, 195-199
21. Parker, E.N., 1979, *Cosmical Magnetic Fields*, (Clarendon Press: Oxford)
22. Chakrabarti, S. K. 1989, *Astrophys. J.*, **347**, 365-372
23. Chakrabarti, S. K. 1990, *Theory of Transonic Astrophysical Flows* (Singapore: World Sci.)
24. Chakrabarti, S. K. 1996, *Astrophys. J.*, **471**, 237-247
25. Chakrabarti, S.K. 1990 *Mon. Not. R. Astron. Soc.* **243**, 610-619
26. Chakrabarti, S. K. 1996, *Astrophys. J.*, **464**, 664-683
27. Chakrabarti, S.K., 1998 in 'Observational Evidence for Black Holes in the Universe', ed. S.K. Chakrabarti (Kluwer Academic Publishers: Dordrecht), 19-48 astro-ph/9807104
28. Chakrabarti, S.K. & Molteni D. 1993, *Astrophys. J.*, **417**, 671-676
29. Molteni, D., Lanzafame, G. & Chakrabarti, S. K. 1994, Simulation of thick accretion disks with standing shocks by smoothed particle hydrodynamics, *Astrophys. J.*, **425**, 161-170

30. Chakrabarti S.K. & Molteni, D. 1995, Mon. Not. R. Astron. Soc. **272**, 80-88
31. Molteni, D., Ryu., D. & Chakrabarti 1996, Numerical Simulations of Standing Shocks in Accretion Flows around Black Holes: A Comparative Study, Astrophys. J., **470**, 460
32. Chakrabarti, S. K., & Titarchuk, L.G. 1995, Astrophys. J., **455**, 623-639
33. Zhang, S.N., Cui, W., Harmon, B.A., Paciesas, W.S., Remillard R.E., & van Paradijs J. 1997, The 1996 Soft State Transition of Cygnus X-1, Astrophys. J., **477**, L95-L100
34. Gilfanov, M., Churazov, E. & Sunyaev, R.A. 1997, Spectral and Temporal variations of the X-ray emission from black hole and neutron star binaries, in *Accretion Disks – New Aspects*, Eds. E. Meyer-Hofmeister & H. Spruit, Springer (Heidelberg)
35. Sunyaev, R.A., et al., 1994, Observations Of X-Ray Novae In Vela 1993 Ophiuchus 1993 And Perseus 1992 Using The Instruments Of The MIR / KVANT Module, Astron. Lett., **20**, 777-784
36. Ebisawa, K. et al. 1994, Spectral evolution of the bright X-ray nova GS 1124-68 (Nova Muscae 1991) observed with Ginga, P.A.S.J., **46**, 375-394
37. Molteni, D., Sponholz, H. & Chakrabarti, S. K. 1996, X-rays from Shock Waves In Accretion Flows Around Black Holes, Astrophys. J., **457**, 805-812
38. Ryu, D., Chakrabarti, S. K., & Molteni, D. 1997, Zero-Energy Rotating Accretion Flows near a Black Hole, Astrophys. J., **474**, 378-388
39. Titarchuk, L.G., Mastichiadis, A., & Kylafis, N. G. 1997, X-Ray Spectral Formation in a Converging Fluid Flow: Spherical Accretion into Black Holes, Astrophys. J., **487**, 834-850
40. Das T. & Chakrabarti S.K. 1997, Astrophys. J. (submitted) astro-ph/9809109
41. Das, T.K. 1998a, 'Observational Evidence for Black Holes in the Universe' ed. S.K. Chakrabarti (Kluwer Academic: Holland) p. 113-122 astro-ph/9807105
42. Das, T.K. 1998b, (this volume)
43. Chakrabarti, S. K. 1998, Indian Journal of Physics, **72B**, 565-569, astro-ph/9810412
44. Chakrabarti, S. K., Titarchuk, L.G., Kazanas, D. & Ebisawa, K. 1996, A & A Supp. Ser., **120**, 163-166
45. Chakrabarti S.K., 1997 Astrophys. J., **484**, 313-322
46. Paul, B., Agrawal, P.C., Rao, A.R., et al., 1998, Quasi-regular X-Ray Bursts from GRS 1915+105 Observed with the IXAE: Possible Evidence for Matter Disappearing into the Event Horizon of the Black Hole, Astrophys. J., **492**, L63-L67
47. Chang, K.M. & Ostriker, J.P. 1985, Standing shocks in accretion flows onto black holes, Astrophys. J., **288**, 428-437
48. Kazanas, D. & Ellison, D. C. 1986, The central engine of quasars and active galactic nuclei Hadronic interactions of shock-accelerated relativistic protons, Astrophys. J., **304**, 178-187
49. Tarafdar, S.P. 1988, A unified formula for mass-loss rate of O to M stars, Astrophys. J., **331**, 932-938
50. Priest, E.R., 1982, Solar Magnetohydrodynamics, (Dordrecht, Holland)
51. Kopp, R.A. & Holzer, T.E., 1976, Dynamics of coronal hole regions. I - Steady polytropic flows with multiple critical points, Sol. Phys., **49**, 43-56
52. Pauldrach, A., Puls, J., and Kudritzki, R.P. 1986, Radiation-driven winds of hot luminous stars - Improvements of the theory and first results, Astr. Ap., **164**, 86-100
53. Chattapadhyay, I 1998, (this volume)
54. Watson, M.G., Stewart, G. C., Brinkann, W., & King, A. R. 1986, Doppler-shifted X-ray line emission from SS433, Mon. Not. R. Astro. Soc., **222**, 261-271
55. Genzel, R., Hollenbach D. & Townes, C.H., 1994, The nucleus of our Galaxy. Rep. Prog. Phys. **57**, 417-479
56. Eckart A. & Genzel, R. 1997, Stellar proper motions in the central 0.1 pc of the Galaxy, Mon. Not. R. Astro. Soc., **284**, 576-598

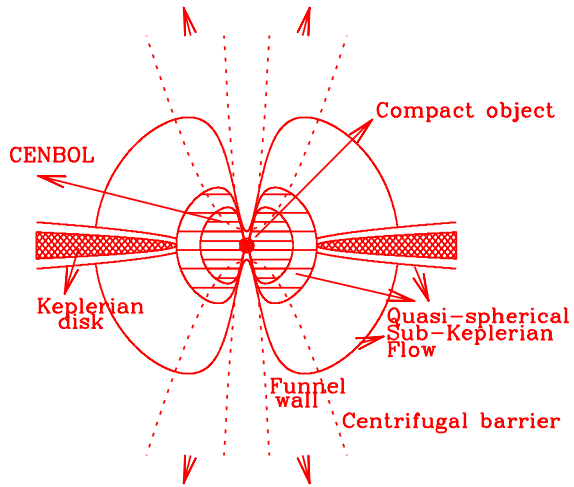
FIGURE CAPTIONS

- Fig. 1** : Classification of the parameter space (central box) in the energy-angular momentum plane in terms of various topology of the black hole accretion. Eight surrounding boxes show the solutions from each of the independent regions of the parameter space. Each small box shows Mach number M against the logarithmic radial distance r (measured in units of GM_{BH}/c^2) Contours are of constant entropy accretion rate \dot{M} . Similar classification is possible for all adiabatic index $\gamma < 1.5$. For $\gamma > 1.5$, only the inner sonic point is possible other than an unphysical ‘O’ type point (Chakrabarti 1996c).
- Fig. 2a** : Cartoon diagram of a very general inflow-outflow configuration of non-magnetized matter around a compact object. Keplerian and sub-Keplerian matter accretes along the equatorial plane. Centrifugally and thermally driven outflows preferentially emerge between the centrifugal barrier and the funnel wall.
- Fig. 2b** Schematic diagram of inflow and outflow around a compact object. Hot, dense region around the object either due to centrifugal barrier or due to plasma pressure effect or pre-heating, acts like a ‘stellar surface’ from which the outflowing wind is developed.
- Fig. 3** Ratio \dot{R}_{in} of the outflow rate and the inflow rate as a function of the compression ratio of the gas at the dense region boundary (solid curve). Also shown in dashed curve is its variation with the polytropic constant n in the strong shock limit. Solid angles subtended by the inflow and the outflow are assumed to be comparable (Chakrabarti 1998a).
- Fig. 4** : Variation of the percentage of mass loss (long dashed curve and right axis) and the energy spectral index α ($F_\nu \propto \alpha^{-\alpha}$) (solid and dotted curves and left axis) with the accretion rate (in units of Eddington rate) of the Keplerian component. Solid curve is drawn when winds are neglected from the advective region and dotted curve includes effect of winds. Overall spectra is softened when the inflow rate is reduced (Chakrabarti 1998b).
- Fig. 5** : Spectra of emitted radiation from the accretion disk with (dotted) and without (solid) effects of winds. Hard X-ray component is softened while keeping soft X-ray bump unchanged (Chakrabarti 1998b).
- Fig. 6** : Few typical solutions which combine accretion and outflow. Input parameters are $\mathcal{E} = 0.0005$, $\lambda = 1.75$ and $\gamma = 4/3$. Solid curve with an incoming arrow represents the pre-shock region of the inflow and the dashed curve with an incoming arrow represents post-shock inflow which enters the black hole after passing through the inner sonic point (I). Dotted curves are the outflows for various γ_o (marked). Open circles are sonic points of the outflowing winds and the crossing point ‘O’ is the outer sonic point of the inflow. The leftmost shock transition (X_{s3}) is obtained from unmodified Rankine-Hugoniot condition, while the other transitions are obtained when the mass-outflow is taken into account.



(a)

Centrifugally and Thermally driven outflows



(b)

